

Numerical Analysis of Hall Thruster Firing Tests

Alexander Bober*

Technion—Israel Institute of Technology, Haifa 32000, Israel

DOI: 10.2514/1.24525

Numerical analysis of the firing tests of several xenon Hall thrusters over the ranges 200–800 V and 0.5–92.7 mg/s anode mass flow rate is presented. The full form of the specific impulse equation is presented. New approximated equations are presented for anode specific impulse and anode efficiency in which a hyperbolic tangent is used as the basic approximating function. Discharge voltage and normalized mass flow are proposed as input performances. The resultant equations characterize small, medium, and large Hall thrusters with the same accuracy. Flow density and normalized mass flow are proposed as scaling factors for correlating anode mass flow rate and thruster geometrical dimensions. Intrathruster parameter values are estimated based on accepted input performances. The ionization degree is shown to be an increasing function of voltage and normalized mass flow. The average voltage ratio is shown to be a decreasing function of voltage. The electron loss parameter is shown to be a decreasing function of voltage and a peculiar V-shaped function of normalized mass flow, with minimums near 50 (mg/s)/m. The average ion charge is shown to be an increasing function of voltage and a parabola-shaped function of normalized mass flow, with maximums near 100 (mg/s)/m. These results will be useful for future analytical investigations.

Nomenclature

D, d	= external and internal diameters of the plasma channel, m, dm, or mm, according to notes
e	= electron charge, C
F	= thrust, N
I_D	= discharge current, A
I_m	= mass current, A, $I_m = e\dot{m}_a/m_i$
I_{sp}	= total specific impulse, m/s
$I_{sp/anode}$	= anode specific impulse, m/s
i	= electron loss parameter (i.e., ratio of electron current to discharge currents)
K_C	= specific impulse coefficient
\dot{m}	= total propellant mass flow rate, mg/s
\dot{m}_a	= anode mass flow rate, mg/s
m_i	= ion or atom mass, kg
P	= power, W
r_i	= ionization degree (i.e., ratio of ion number leaved thruster to atom number entered plasma channel at the same time)
U	= discharge voltage, V
U_c	= cathode voltage loss, V
U^*	= average accelerating voltage, V
Z	= average ion charge in electron charge units
η_t	= thrust efficiency
$\eta_{t/anode}$	= anode efficiency

Introduction

AN ELABORATE thought is presented in one of the basic works in the electric propulsion community: “Physical processes in stationary plasma thrusters [one type of Hall thruster] are extremely complicated, despite the simple construction of the devices” [1]. Many electric propulsion teams have executed effective, detailed, and complicated investigations; nevertheless, it is evident that Hall thruster performances can be improved through further analytical and experimental research.

Received 9 April 2006; revision received 30 November 2006; accepted for publication 3 January 2007. Copyright © 2007 by the American Institute of Aeronautics and Astronautics, Inc. All rights reserved. Copies of this paper may be made for personal or internal use, on condition that the copier pay the \$10.00 per-copy fee to the Copyright Clearance Center, Inc., 222 Rosewood Drive, Danvers, MA 01923; include the code 0748-4658/07 \$10.00 in correspondence with the CCC.

*Senior Scientist, Asher Space Research Institute; bas@technion.technion.ac.il.

In this paper, an attempt is made to find new interdependences between input and output thruster performances, including intrathruster parameters on the basis of 1) analysis of simple basic Hall thruster definitions and 2) numerical analysis of the results of some firing tests of xenon Hall thrusters, namely, stationary plasma thrusters.

Basic Formulas

The electrical thruster definitions for specific impulse and thrust efficiency are commonly known:

$$I_{sp} = \frac{F}{\dot{m}}; \quad I_{sp/anode} = \frac{F}{\dot{m}_a} \quad (1)$$

$$\eta_t = \frac{\dot{m} I_{sp}^2}{2P}; \quad \eta_{t/anode} = \frac{\dot{m}_a I_{sp/anode}^2}{2P} \quad (2)$$

where \dot{m} is the sum of the anode-mass-flow-rate-entered anode and the cathode-mass-flow-rate-entered cathode. There are two ways to analyze the thruster: 1) using the left-hand sides of Eqs. (1) and (2) to study the whole thruster or 2) using the right-hand sides of Eqs. (1) and (2) to analyze the intrathruster processes. Consumptions of power and propellant concerned with the cathode are not taken into account in this paper; the second way is used here. $I_{sp/anode}$ can be presented as a function of discharge voltage and a coefficient:

$$I_{sp/anode} = \sqrt{\frac{2eU}{m_i}} K_C \quad (3)$$

The equation for the coefficient K_C can then be obtained from Eqs. (2) and (3), as follows:

$$K_C = \eta_{t/anode} \frac{I_D}{I_m} \quad (4)$$

The specific impulse equation can then be presented as follows:

$$I_{sp/anode} = \sqrt{\frac{2eU}{m_i}} \eta_{t/anode} \frac{I_D}{I_m} \quad (5)$$

Thus, the anode specific impulse is shown to be a function of discharge voltage, anode efficiency, and current ratio I_D/I_m . It is known that the current ratio characterizes current flowing within the plasma channel. It is a common function of ion and electron currents. Equation (5) allows interrelating intrathruster parameters r_i , Z ,

U^*/U , and i and dimensionless factors $\eta_{t/\text{anode}}$, I_D/I_m , and $K_C = I_{\text{sp}/\text{anode}}^2/(2eU/m_i)$. The dimensionless factors are calculated on the basis of thruster performances measured directly. A thruster quality can then be characterized by two of three dimensionless values: thrust efficiency, discharge and mass currents ratio, and coefficient K_C .

The ionization and acceleration processes within the Hall thruster chamber (or plasma channel) are determined by at least four intrathruster parameters [2]: 1) ionization degree, 2) average ion charge, 3) average accelerating voltage, and 4) electron loss parameter.

The average ion charge is given by [3]

$$Z = 1 + \frac{\text{Xe}^{2+}\text{fraction}}{\dot{m}_a/m_i} + \frac{2\text{Xe}^{3+}\text{fraction}}{\dot{m}_a/m_i} + \dots \quad (6)$$

The electron loss parameter is a ratio of electron current to discharge current at the thruster exit (i.e., when the ionization process has ended).

Clearly, natural limitations of intrathruster parameters exist: $r_i \leq 1$, $Z \geq 1$, $U^* \leq U$, and $i \geq 0$. The following expressions [3] can be obtained for the flow of Z -charged ions with the ion flow rate $r_i \dot{m}_a/m_i$ exhausted from a thruster under the influence of U^* voltage:

$$I_D = \frac{er_i Z \dot{m}_a}{m_i(1-i)} \quad (7)$$

$$F = r_i \dot{m}_a \sqrt{\frac{2eZU^*}{m_i}} \quad (8)$$

where I_D and F are firing test results measured directly. Interdependences between the intrathruster parameters and the dimensionless values K_C , $\eta_{t/\text{anode}}$, and I_D/I_m are given by [3]

$$K_C = r_i^2 Z \frac{U^*}{U} \quad (9)$$

$$\eta_{t/\text{anode}} = r_i(1-i) \frac{U^*}{U} \quad (10)$$

$$\frac{I_D}{I_m} = \frac{r_i Z}{1-i} \quad (11)$$

Experimental Data Analysis

Three input values characterize Hall thruster output performances: discharge voltage, anode mass flow rate, and the external diameter of the plasma channel. Clearly, other dimensions of a rational thruster design should correspond with D .

In this paper, we will find interdependences between input and output xenon stationary plasma thruster (SPT) parameters on the basis of the preceding expressions and experimental data over the ranges of 200–800 V and 0.5–92.7 mg/s anode mass flow rate. Experimental data analyzed here are chosen from publicly available papers. These are the results of 126 firing tests of five large and medium thrusters [4–8] and four small thrusters [9–12] over the range of external plasma channel diameter from 28 to 457 mm. The accuracy measurement estimation of analyzed data was not executed. The usual accuracy of measurement is ± 2 –3% for power, thrust, and mass flow rate. This experimental accuracy leads to ± 0.05 uncertainties in anode efficiency and ± 3 –5% uncertainties in the anode specific impulse.

Attempts are made to find simple zoom power dependence between thruster dimensions and rational propellant mass flow [13,14]. Rational propellant mass flow rate and discharge voltage are not points for a good thruster. A wide range of operating conditions inheres in a rational thruster. It is possible to assume that acceptable

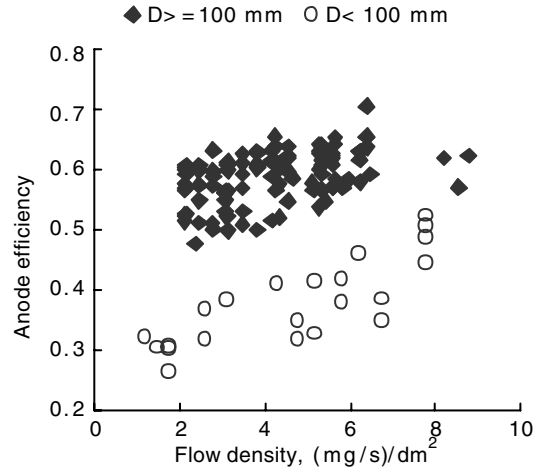


Fig. 1 Anode efficiency vs flow density.

mass flow is determined by neutral atom concentration near the anode. The concentration should be a necessary and ample value for effective ionization process at the selected voltage. The following inference can be noted on the basis of total experience. Acceptable thruster performances are observed over the following range of anode mass flow:

$$2 \text{ (mg/s)/dm}^2 \sim \leq \frac{\dot{m}_a}{\pi D^2/4} \sim \leq 10 \text{ (mg/s)/dm}^2 \quad (12)$$

Presented borders are not precise values. Special tests are needed for their accurate definition. However such borders exist, beyond any doubt. Presented limiting values will be taken into account in this paper.

The noticeable difference between small and larger thrusters exists at the same flow density $\dot{m}_a/(\pi D^2/4)$. Experimental results [4–12] shown in Fig. 1 demonstrate the difference. In this paper, another argument is proposed instead of flow density. It is normalized mass flow \dot{m}_a/D (see Fig. 2).

In this case, the continuous interdependence between anode efficiency and normalized mass flow shows up with abrupt degradation of anode efficiency near a normalized mass flow of 25 (mg/s)/m and less. It should be noted that a similar value has been proposed [15] as a plasma thruster analogy parameter.

It is possible to assume that the operation mode area at a flow density of 2...10 (mg/s)/dm² includes a certain “risky zone” in which normalized mass flow is less than 25 (mg/s)/m or 0.025 (mg/s)/mm. Such a diagram is presented in Fig. 3.

Thruster performances become notably worse when selected values of anode mass flow rate and external plasma channel diameter

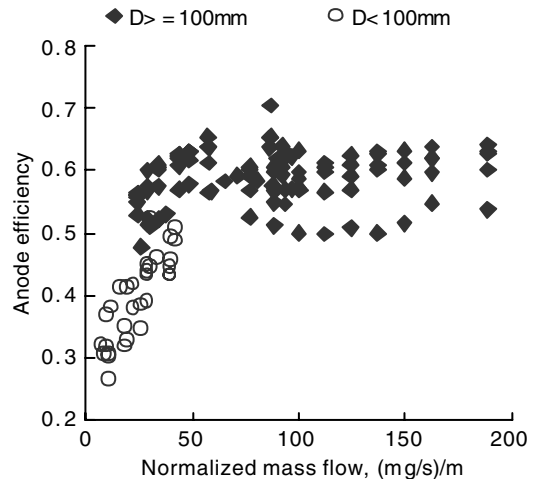


Fig. 2 Anode efficiency vs normalized mass flow.

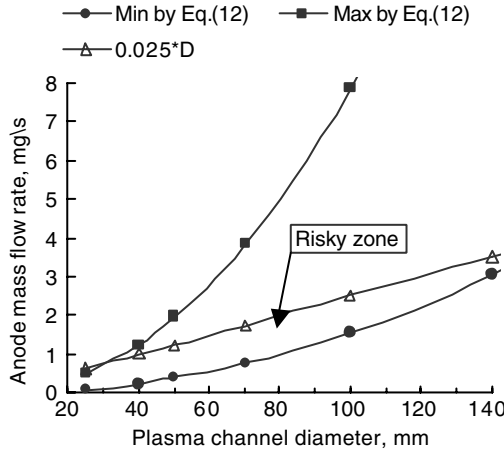


Fig. 3 Operation area for SPT using xenon.

are within the risky zone. The risky zone is absent if $D > \sim 140$ mm. Possible reasons of existence of such a zone will be analyzed later. The flow density and the normalized mass flow can be defined as factors ascertaining correlation of rational values of propellant mass flow rate and thruster geometrical dimensions. It is possible to think that the flow density determines the initial ionization process near the anode and the normalized mass flow, which are processes of ionization and acceleration later.

Anode specific impulse and anode efficiency equations are a function of discharge voltage and normalized mass flow. Acceptable approximated interdependences between the input and output parameters of the xenon stationary plasma thruster will be found. The acceptable interdependences should agree with output performance behavior over the wide range of normalized mass flow from ~ 15 (mg/s)/m up to ~ 250 (mg/s)/m. As a rule, power dependences are used for the purpose of approximating in the electric propulsion community. Using the experimental data [4–12], the following approximated power equations are obtained for estimation of the analyzing ranges of discharge voltage and normalized mass flow:

$$I_{sp/anode} = \sqrt{\frac{2eU}{m_a}} \times U^{0.085} (\dot{m}_a/D)^{0.074} \quad (13)$$

$$\eta_{t/anode} = 0.071 U^{0.324} (\dot{m}_a/D)^{0.01} \quad (14)$$

Comparison of the experimental data [4–12] and the estimation is presented in Figs. 4–6.

The following conclusions can be made as a result of visual analysis of the presented diagrams. Accordance of experimental and

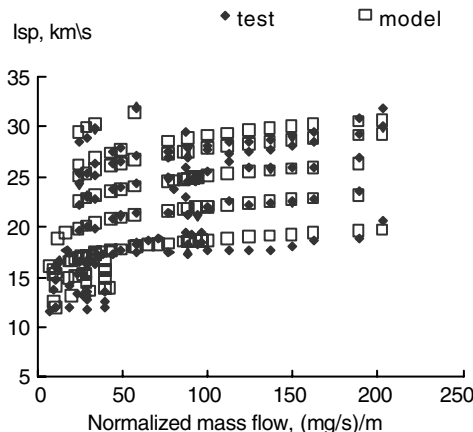


Fig. 4 Anode specific impulse vs normalized mass flow; model is calculated by Eq. (13).

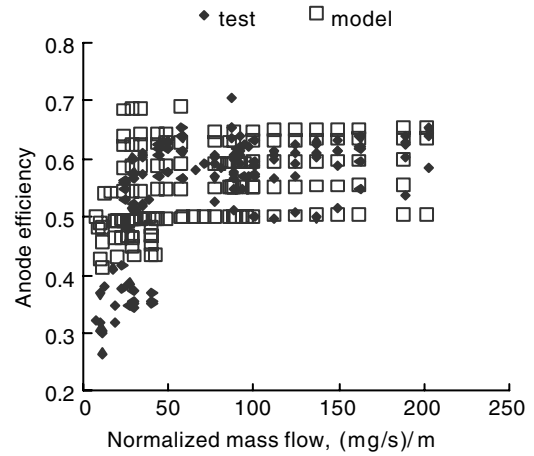


Fig. 5 Anode efficiency vs normalized mass flow; model is calculated by Eq. (14).

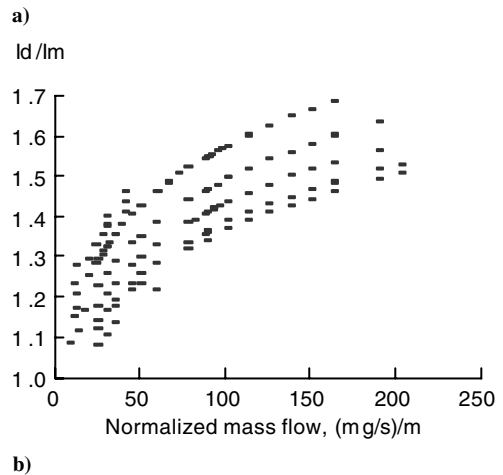
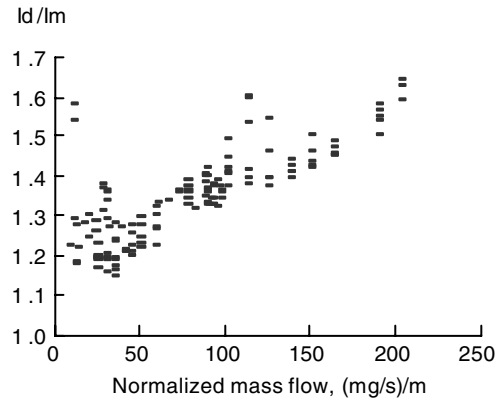


Fig. 6 Current ratio I_D/I_m vs normalized mass flow: a) experimental data [4–12] and b) model calculated by Eqs. (4), (13), and (14).

model data of anode specific impulse is acceptable. Model data of anode efficiency do not conform to the experimental data at small values of normalized mass flow. The abrupt decrease of anode efficiency is absent in the model. Such a model cannot be used for serious analysis. General forms of the experimental and model data of current ratio I_D/I_m do not conform to each other. The experimental dependence is a V-shaped function with a minimum near 25 (mg/s)/m. The model dependence is a monotone decreasing function. A consequent analysis is impossible with such a model. The only power dependence cannot be used for analysis of both large and small thrusters. There are no critical reasons to divide analyses of small and large thrusters. The basic approximated function should be

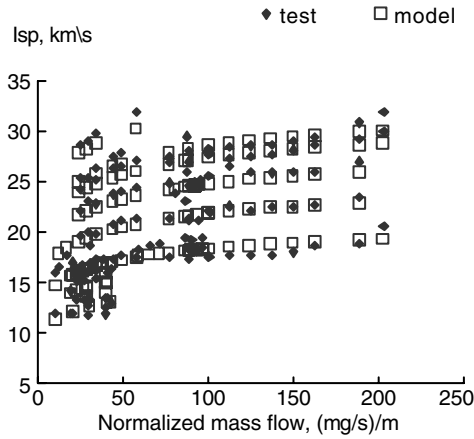


Fig. 7 Anode specific impulse vs normalized mass flow; model is calculated by Eq. (16).

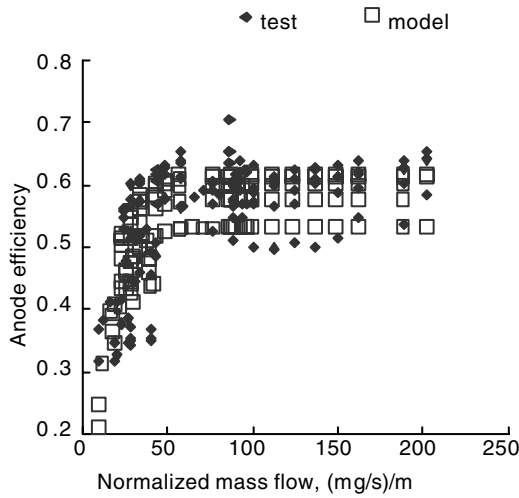


Fig. 8 Anode efficiency vs normalized mass flow; model is calculated by Eq. (17).

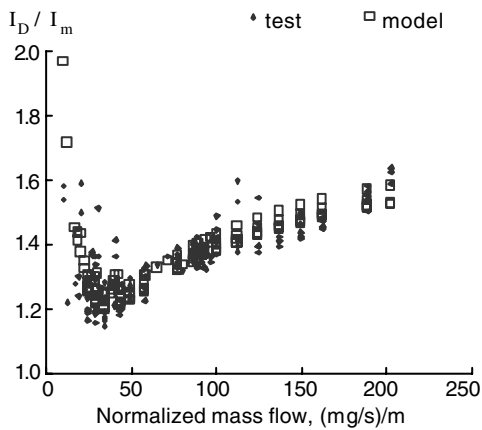


Fig. 9 Current ratio I_D/I_m vs normalized mass flow; model is calculated by Eqs. (4), (16), and (17).

changed. The hyperbolic tangent is proposed in this paper. This function is monotone, increasing from zero to one when the argument is changed from zero to infinity. Such behavior simulates the real behavior of K_C and $\eta_{I/\text{anode}}$, as shown by the experiments.

A hyperbolic tangent is the combination of the two exponents, increased and decreased, as follows:

$$\text{th}(x) = (e^x - e^{-x}) / (e^x + e^{-x}) \quad (15)$$

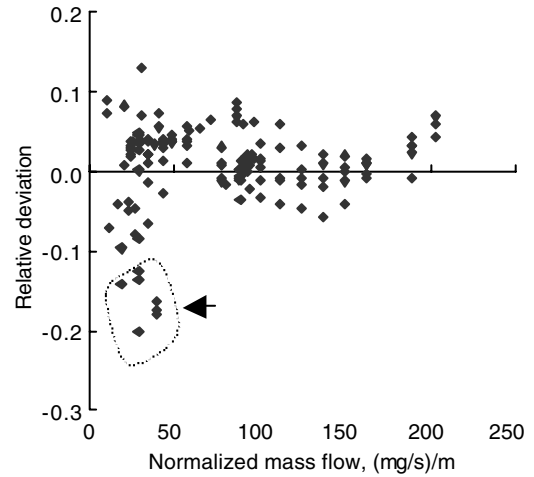


Fig. 10 Anode specific impulse: relative deviation between test and model data from Fig. 7.

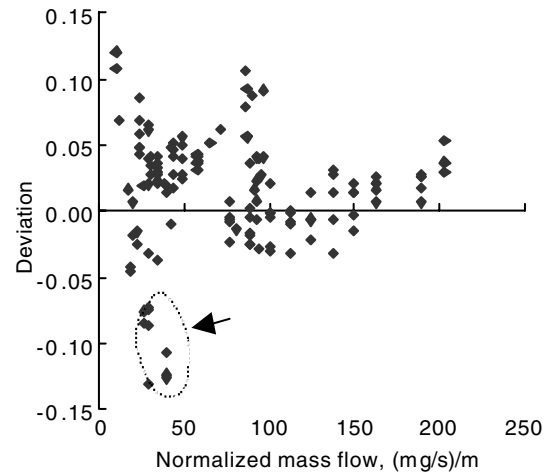


Fig. 11 Anode efficiency: deviation between test and model data from Fig. 8.

Many thermodynamic and electromagnetic processes have exponential behavior.

Using ordinary approximated methods, the following equations are obtained:

$$I_{sp/\text{anode}} = \sqrt{\frac{2eU}{m_i} \left\{ \left[\text{th}\left(\frac{U}{300}\right) \right]^{0.5} \left[\text{th}\left(\frac{\dot{m}_a/D}{200}\right) \right]^{0.2} \right\}} \quad (16)$$

$$\eta_{I/\text{anode}} = 0.625 \left[\text{th}\left(\frac{U}{300}\right) \right]^{0.6} \text{th}\left(\frac{\dot{m}_a/D}{20}\right) \quad (17)$$

where the braces indicate K_C .

Comparisons of test results [4–12] and estimations are presented in Figs. 7–9. General forms of experimental and model data coincide with each other satisfactorily. Anode specific impulse and anode efficiency are an increasing function of normalized mass flow. The current ratio is a peculiar V-shaped function of normalized mass flow with a minimum near 25 (mg/s)/m.

Deviations between the experimental data and the estimations are presented in Figs. 10–12. The deviations do not far exceed the usual experimental uncertainties. The received conformity of calculation and experiment is enough for finding of intrathruster parameter behavior. The resultant equations characterize small, medium, and large thrusters with the same accuracy. Arrows mark some differing points that are the results of firing tests of the only thruster [12].

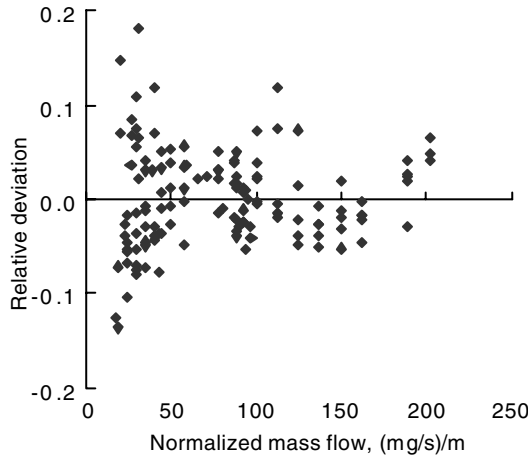


Fig. 12 Current ratio I_D/I_m ; relative deviation between test and model data from Fig. 9.

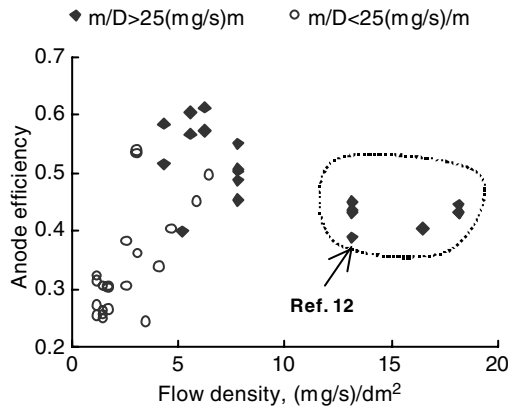


Fig. 13 Anode efficiency [9–12] vs flow density.

Comparison between anode efficiency values of analyzing low power thrusters [9–12] is presented in Fig. 13.

Values of the flow density of the noted thruster at presented operation modes [12] exceed the approved border of ~ 10 (mg/s)/dm². The total experience demonstrates that anode efficiency is decreased in those cases, electrical oscillations are increased, and thermal difficulties with hard lifetime problems appear. However, similar attempts can enlarge common knowledge in the Hall thruster community.

The considerable difference between experimental and model data at normalized mass flow is less than ~ 15 (mg/s)/m. That is not important, because applications of such small values are not advisable.

Thus, successful hyperbolic tangent application can be acknowledged for the purpose of approximating here. Proposing approximated equations demonstrate that the current ratio I_D/I_m increases at small values of normalized mass flow. Such an effect has long been observed experimentally.

Unaccounted Factors

Three unaccounted factors can be noted here.

The first factor is intrathruster magnetic field configuration. Generally speaking, two parameters are required for perfect analysis: the magnetizing force at the exit plane and its gradient along the plasma channel axis.

The second factor is the d/D ratio. As a rule, the value of d/D is near 0.6 for many thrusters. An interesting problem is to determine the d/D influence on thruster performances, which should be a subject of future study. Clearly, plasma channel length is also an interesting factor.

The third factor is the so-called cathode voltage loss (i.e., the potential difference between the exit plane and the cathode). It is

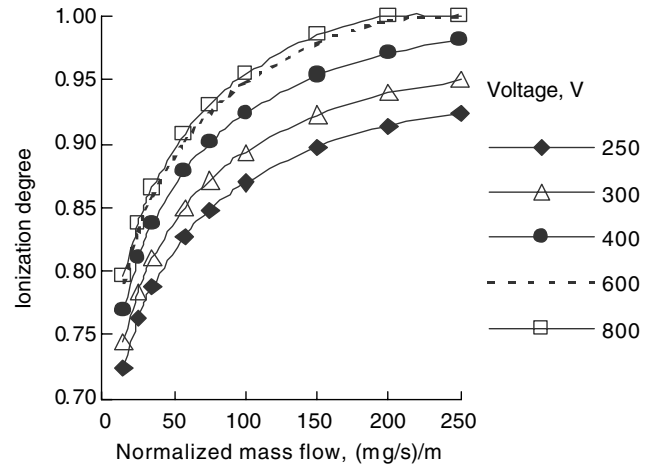


Fig. 14 Ionization degree; averaged values at four selected points.

possible to think that this part of voltage does not take part in ion acceleration. Rational selection of the cathode model can improve thruster performances considerably [16,17]. Large cathodes are used for the initial firing tests of small thrusters in many cases, which is a mistake. Clearly, anode specific impulse and anode efficiency can be calculated, with the exception of cathode mass flow rate. Still, a small cathode will be used when adjusting firing tests afterward. It is clear that cathode voltage loss will increase in that case (i.e., the average accelerating voltage will decrease, with inevitable fatal consequences). As shown in [16], the cathode voltage loss value can be 5–40 V. It appears that $U - U_C$ should be used in formulas, in place of the discharge voltage, but that is a special problem.

Intrathruster Parameters

Intrathruster parameters r_i , Z , U^*/U , and i at the thruster exit depend on input data U , \dot{m}_a , and D . They can be obtained according to considerations already presented.

The values of ionization degree and electron loss parameter can be calculated for four points:

$$\begin{aligned} (Z = 1; U^*/U = 0.75), & \quad (Z = 1; U^*/U = 0.9) \\ (Z = 1.3; U^*/U = 0.75), & \quad (Z = 1.3; U^*/U = 0.9) \end{aligned}$$

For first approximation, it is assumed that these points correspond with limiting possibilities of real ionization process within the Hall thrusters. Results obtained from Eqs. (9–11), (16), and (17) are presented in Figs. 14 and 15.

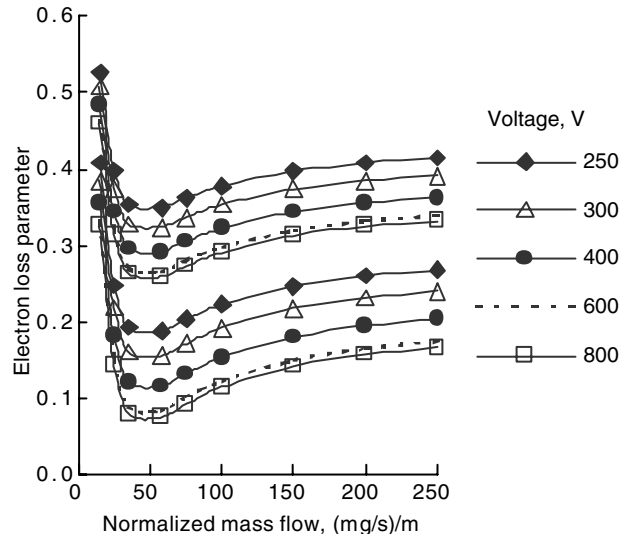


Fig. 15 Electron loss parameter: maximum and minimum values at four selected points.

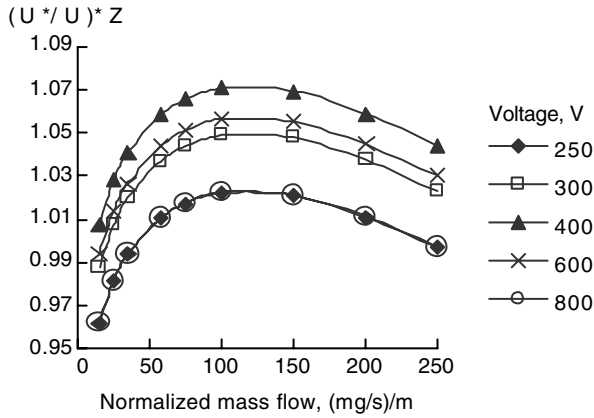


Fig. 16 Product $(U^*/U) \cdot Z$ vs normalized mass.

The result is presented in Fig. 14. Ionization degree is shown to be a monotone increasing function of voltage and normalized mass flow.

Electron loss parameter curves are similar to current ratio dependence. They are shown to be a decreasing function of voltage and a peculiar V-shaped function of normalized mass flow, with a minimum near 50 (mg/s)/m. The electron loss increase at small values of normalized mass flow can be explained by the presence of secondary electron emission from dielectric walls in the SPT. It is possible to assume that the value of secondary electron emission mainly depends on the size of the dielectric walls. The number of electrons created by atom ionization is decreased because of normalized mass flow decrease. Although the number of secondary emitted electrons is not changed, their share in the discharge current is increased. Finally, the value of the electron loss parameter is increased. It is possible to think that I_D/I_m dependence on normalized mass flow has another view in a thruster with metal walls when secondary electron emission is absent. Intrathruster electron current is the sum of three electron flows: 1) electrons created at atom ionization, 2) electrons that entered the plasma channel from the cathode, and 3) secondary electron emission. The presented complicated dependence in Fig. 15 deserves deep analysis.

The obtained ionization degree data in Fig. 14 can be approximated as follows:

$$r_i = 0.37U^{0.08}(\dot{m}_a/D)^{0.08} \quad (18)$$

The product average ion charge and average accelerating voltage can now be calculated from Eqs. (9), (16), and (18). Results are presented in Fig. 16.

The surface presented in Fig. 16 is shown to be a curved trough-shaped profile, with $(U^*/U) \cdot Z$ maximums near 400 V and 100 (mg/s)/m.

The values of the average voltage ratio U^*/U can now be calculated on the basis of the experimental data [17] at mass flow rate 10 mg/s (i.e., normalized mass flow is 57.8 (mg/s)/m in that case). The Z values calculated by Eq. (6) are [17] 1.075, 1.11, 1.14, and 1.18 for discharge voltages of 300, 400, 600, and 800 V, respectively.

The average voltage ratio U^*/U is calculated by the product $(U^*/U) \cdot Z$ from Fig. 16 and the Z data just described, results are presented in Fig. 17. The average voltage ratio U^*/U is decreased when the discharge voltage is increased. When first estimating, the obtained average accelerating voltage values can be used for all values of normalized mass flow. The values of the average ion charge can now be calculated from Eqs. (9) and (16). The results of the calculations are presented in Figs. 18 and 19. Cross sections of the obtained surface are presented at constant values of voltage and

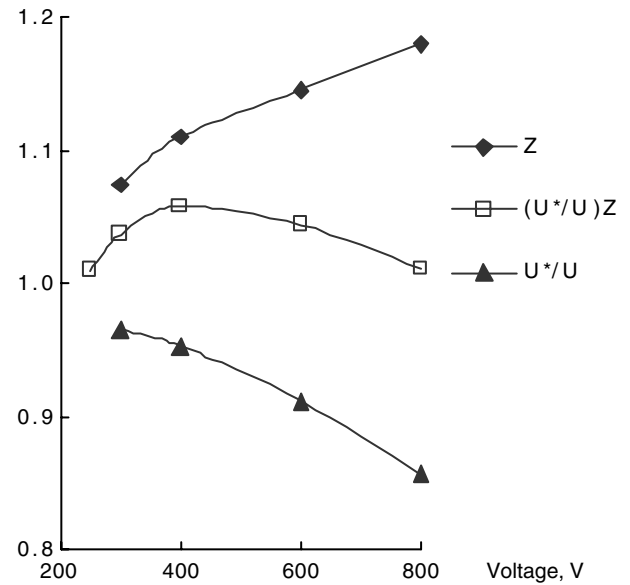


Fig. 17 Average voltage ratio U^*/U determination.

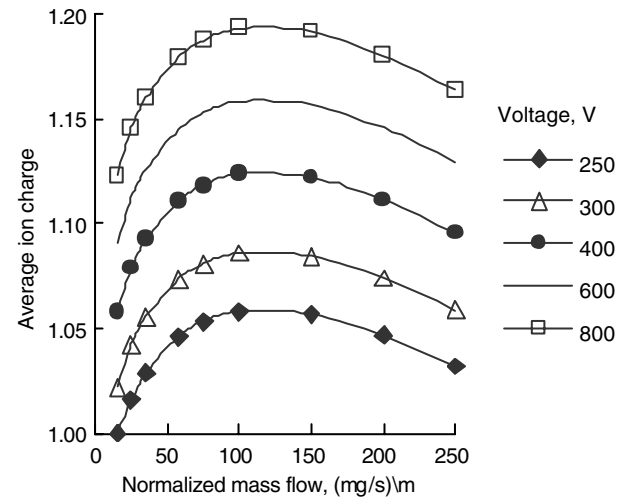


Fig. 18 Cross sections of average ion charge surface.

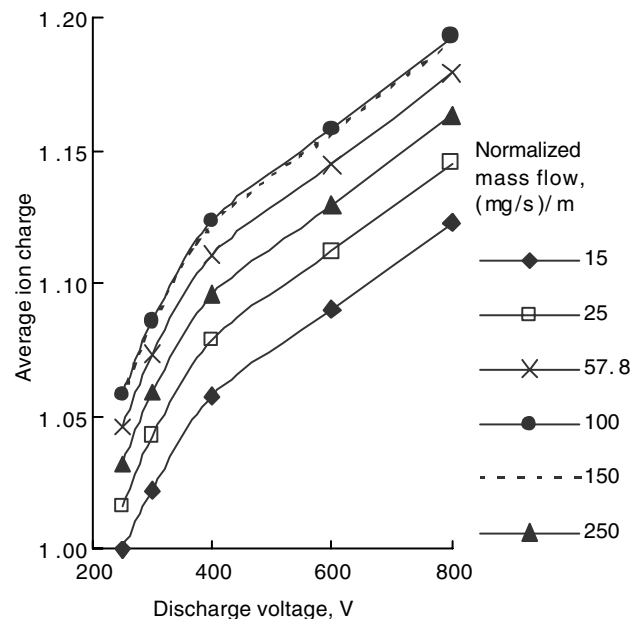


Fig. 19 Cross sections of average ion charge surface.

Table 1 Average ion charge based on the data.

Discharge voltage, V	300	400	600	800
Average ion charge	1.075	1.11	1.14	1.18

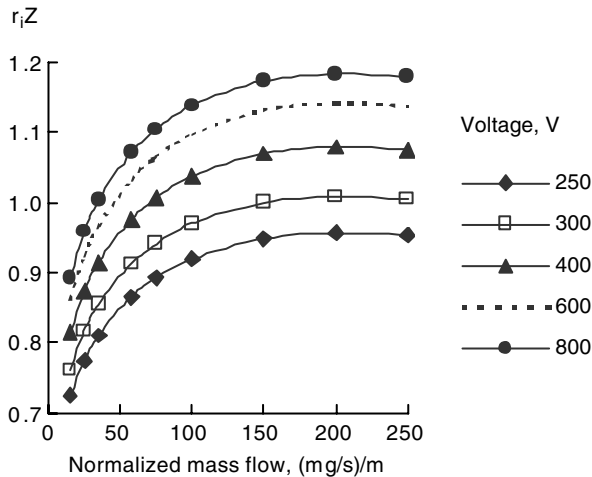


Fig. 20 Product $r_i Z$ vs normalized mass flow.

normalized mass flow. The average ion charge is shown to be an increasing function of discharge voltage and a parabola-shaped function of normalized flow, with maximums near 100 (mg/s)/m. In spite of the fact that the average ion charge is decreased at large normalized mass flow, product $r_i Z$ (proportionate to the total ion charge) is an increasing function of normalized mass flow (see Fig. 20).

The presented data deserve deep analytical investigations.

Conclusions

1) An analysis of plasma thruster basic formulas demonstrates that anode specific impulse is a function of the discharge voltage, anode efficiency, and current ratio I_D/I_m . The current ratio characterizes current flowing within the plasma channel. It is a common function of ion and electron currents. The presented equation allows interrelating intrathruster parameters r_i , Z , U^*/U , and i and dimensionless factors $\eta_{t/\text{anode}}$, I_D/I_m , and $K_C = I_{sp}^2/(2eU/m_i)$. The dimensionless factors are calculated on the basis of thruster performances measured directly.

2) New approximated equations are proposed for xenon Hall thruster performances. A hyperbolic tangent is used as a basic approximated function. U and normalized mass flow \dot{m}_a/D are proposed as input performances. The resultant equations characterize small, medium, and large thrusters with the same accuracy. The flow density $\dot{m}_a/(\pi D^2/4)$ and the normalized mass flow can be defined as factors ascertaining correlation of rational values of propellant mass flow rate and thruster geometrical dimensions. Many firing tests demonstrate acceptable density flow over the range $\sim 2 \sim 10$ (mg/s)/dm². Still, thruster performances become worse at normalized mass flow of less than ~ 25 (mg/s)/m. Normalized mass flow is a *limiting factor* when $D \sim < 140$ mm. It is possible to think that the flow density determines the ionization process near the anode and the normalized mass flow, which are processes of ionization and acceleration later.

3) Values of three dimensionless parameters are presented on the basis of experimental data. Anode specific impulse and anode efficiency are increasing functions of normalized mass flow. Current ratio I_D/I_m is a peculiar V-shaped function of normalized mass flow, with minimums near 25 (mg/s)/m.

4) Estimated values of four intrathruster parameters are presented. They are calculated on the basis of basic formulas and obtained approximation. Average ion charge values obtained experimentally

at a normalized mass flow of 57.8 (mg/s)/m were also used. Ionization degree r_i is shown to be a monotone increasing function of voltage and normalized mass flow. Electron loss parameter i curves are similar to current ratio dependence. They are shown to be a decreasing function of voltage and a peculiar V-shaped function of normalized mass flow, with a minimum near 50 (mg/s)/m. The average voltage ratio U^*/U is decreased when the discharge voltage increases. The average ion charge Z is shown to be an increasing function of voltage and a parabola-shaped function of normalized mass flow, with maximums near 100 (mg/s)/m. Obtained results will be useful for future analytical investigations.

Acknowledgments

The author wishes to thank Asher Space Research Institute Director M. Guelman and N. Miller from RAFAEL for the opportunity to study electric propulsion.

References

- [1] Morozov, A. I., and Savelyev, V. V., *Reviews of Plasma Physics*, Kluwer Academic, New York, Vol. 21, 2000, p. 203.
- [2] Hofer, R. R., and Jankovsky, R. S., "A Hall Thruster Performance Model Incorporating the Effects of a Multiply-Charged Plasma," AIAA Paper 2001-3322, July 2001.
- [3] Bober, A., "Hall-Effect Thruster Estimation of Intra-Thruster Performances," *Proceedings of the 4th International Spacecraft Propulsion Conference*, SP-555, ESA, Paris, 2004.
- [4] Manzella, D. H., Jankovsky, R. S., and Hofer, R. R., "Laboratory Model 50 kW Hall Thruster," AIAA Paper 2002-3676, July 2002.
- [5] Jankovsky, R., McLean, C., and McVey, J., "Preliminary Evaluation of a 10 kW Hall Thruster," AIAA Paper 99-0456, Apr. 1999.
- [6] Hofer, R. R., "Development and Characterization of High-Efficiency, High-Specific Impulse xenon Hall Thrusters," NASA CR-2004-213099, June 2004.
- [7] Manzella, D., Hamley, J., Miller, J., Clauss, C., Kozubsky, K., and Gnizdor, R., "Operational Characteristics of the SPT-140 Hall Thruster," AIAA Paper 97-2919, July 1997.
- [8] Manzella, D., Jacobson, D., and Jankovsky, R., "High Voltage SPT Performance," AIAA Paper 2001-3774, Nov 2001.
- [9] Raitses, Y., Guelman, M., Ashkenazy, J., and Appelbaum, G., "Orbit Transfer with a Variable Thrust Hall Thruster Under Drag," *Journal of Spacecraft and Rockets*, Vol. 36, No. 6, 1999, pp. 875–881.
- [10] Manzella, D., Sankovic, J., Haag, T., Semkin, A., and Kim, V., "Evaluation of Low Power Hall Thruster Propulsion," AIAA Paper 96-2736, July 1996.
- [11] Belikov, M. B., Gorshkov, O. A., Jakupov, A. B., and Khartov, S. A., "Experimental Research of SPT Low-Power Perspective Model," AIAA Paper 98-3786, 1998.
- [12] Azziz, Y., "Instrument Development and Plasma Measurements on a 200-Watt Hall Thruster Plume," M.S. Thesis, Massachusetts Inst. of Technology, Cambridge, MA, Sept. 2003, p. 123.
- [13] Biagioni, L., Saverdi, M., and Andrenucci, M., "Scaling and Performance Prediction of Hall Effect Thrusters," AIAA Paper 2003-4727, July 2003.
- [14] Yu Daren, Ding Yongjijie, and Zeng Zhi, "Improvement of the Scaling Theory of the Stationary Propulsion Thruster," *Journal of Propulsion and Power*, Vol. 21, No. 1, 2005, pp. 139–143.
- [15] Bugrova, A. I., Lipatov, A. C., Morozov, A. I., and Churbanov, D. V., "On One Analogy Parameter of Plasma Accelerators SPT-Type," *Technical Physics Letters*, Vol. 28, No. 19, 2002, pp. 56–61.
- [16] Oranskiy, A. I., "Perspective Cathodes of Electrical Thrusters," *Aerospace Engineering and Technology*, Vol. 8, No. 16, 2004, pp. 178–185 (in Russian).
- [17] Hofer, R. R., and Gallimore, A. D., "Efficiency Analysis of a High-Specific Impulse Hall Thruster," AIAA Paper 2004-3602, July 2004.

G. Spanjers
Associate Editor